

# Damage thresholds for cultured retinal pigment epithelial cells exposed to lasers at 532 nm and 458 nm

**Michael L. Denton**

**Michael S. Foltz**

**Kurt J. Schuster**

Northrop Grumman  
Warfighter Concepts and Applications  
Department  
San Antonio, Texas 78228

**Larry E. Estlack**

Conceptual MindWorks, Inc.  
San Antonio, Texas 78228

**Robert J. Thomas**

AFRL/HEDO  
Air Force Research Laboratory  
Brooks City-Base, Texas 78235

**Abstract.** The determination of safe exposure levels for lasers has come from damage assessment experiments in live animals, which typically involve correlating visually identifiable damage with laser dosimetry. Studying basic mechanisms of laser damage in animal retinal systems often requires tissue sampling (animal sacrifice), making justification and animal availability problematic. We determined laser damage thresholds in cultured monolayers of a human retinal pigment epithelial (RPE) cell line. By varying exposure duration and laser wavelength, we identified conditions leading to damage by presumed photochemical or thermal mechanisms. A comparison with literature values for ocular damage thresholds validates the *in vitro* model. The *in vitro* system described will facilitate molecular and cellular approaches for understanding laser-tissue interaction. © 2007 Society of Photo-Optical Instrumentation Engineers. [DOI: 10.1117/1.2737394]

Keywords: laser-induced damage; cells; photothermal; photochemical.

Paper 06337R received Nov. 27, 2006; revised manuscript received Feb. 16, 2007; accepted for publication Mar. 6, 2007; published online May 10, 2007.

## 1 Introduction

To provide guidelines for eye-safe exposure to lasers, the laser safety community has relied mainly on damage assessment in nonhuman primate studies. Results of *in vivo* studies have shown that laser damage in the retina depends upon wavelength, power level, and duration of the exposure.<sup>1,2</sup> Histopathologic analysis of retinal damage indicates that damage to the retinal pigment epithelial (RPE) cells, due to absorption by intracellular melanosomes, is universal in all three known mechanisms leading to laser-induced lesion formation.<sup>1,3</sup> Thus, pigmentation plays an important role in laser absorption and damage.

Analyzing trends in damage threshold data can provide information regarding mechanisms, as described in the review by Stuck.<sup>4</sup> The familiar action spectrum, relating threshold to incident laser wavelength, illustrates a dramatic increased efficacy in the blue and ultraviolet region of the spectrum, indicating a transition to a photochemical (actinic) mechanism. Distinguishing trends can also be found when relating threshold (laser radiant exposure) to exposure duration on log-log axes, an analysis we describe as the “temporal action profile.” Thermal damage mechanisms are thought to predominate for the shorter exposures, where there is a nonlinear increase (power function) in threshold radiant exposure with increasing exposure time. At longer exposure durations (especially for actinic wavelengths), the trend is for the threshold radiant exposure to remain constant with increasing exposure duration. This identifies the principle of reciprocity, whereby a

reciprocal relationship exists between threshold irradiance and exposure duration.<sup>5,6</sup> In the transitional phase between these opposing trends (around 20 s), there is most likely a complex interplay of both thermal and chemical outcomes.

Over the years, there have been theoretical models developed to describe photothermal damage,<sup>7,8</sup> and the *in vivo* threshold data has played a vital role in validating these models. Specifically, computer-simulated retinal temperature rises, coupled with the generally accepted temperature dependence for the denaturation of proteins, has provided support to the basic data trends in temporal action profiles as to when damage mechanisms transition from thermal to photochemical.<sup>2,4</sup> Currently, there are no computer modeling and simulation programs that accurately predict photochemical damage. Biochemical analysis of ocular lesions is needed to identify key components, such as reactive oxygen species (ROS), responsible for photochemical injury. Once time-dependent and wavelength-specific components are identified, a rate-process approach to modeling and simulation can proceed. Even with the utility of *in vivo*-based laser-capture microdissection,<sup>9</sup> the prospect of biochemically analyzing sufficient biomaterial of a retinal-visible lesion generated in the intact eye is an arduous task. A simple *in vitro* RPE model system, if found to respond to lasers in similar fashion to RPE cells *in vivo*, could lead to validation of modeling refinements and provide ample tissue for proteomic and transcriptomic analysis.

In the present work, we have used our previously described<sup>9</sup> *in vitro* cell model to measure estimated dose for 50% lethality (ED<sub>50</sub>) thresholds for four exposure durations at two different wavelengths, twice varying the melanosome

Address all correspondence to Dr. Robert J. Thomas, 2624 Louis Bauer Drive, Brooks City-Base, TX 78235. Tel: 210-536-6558; Fax: 210-536-3903; E-mail: robert.thomas@brooks.af.mil

density within the cells. We show that although the absolute values of the thresholds differ from minimal visible lesion (MVL) data taken from the literature, we see trends in the temporal action profile that are consistent with that from ocular exposures in rhesus monkeys. We also note that our analysis of 532-nm exposures precedes safety studies in animals. Overall, this is a second validation of the *in vitro* model and a starting point for both refining existing computer models and identifying interesting laser exposures to study at the molecular level.

## 2 Materials and Methods

### 2.1 Cell Culture and Damage Assessment

A full description of the cell culture system used in our laser bioeffects experiments, including artificial pigmentation with exogenous melanosome particles (MP), preparation for laser exposure in microtiter plates, and the determination of laser damage by cytochemical assays, has been previously described.<sup>10,11</sup> The only differences from the prior study are that we now use 96-well microtiter plates, and we have included an additional pigmentation density (equivalents of 160 MP/cell and 1600 MP/cell). Briefly, stock cultures of hTERT-RPE1, a human-derived retinal pigment epithelial cell line (BD Biosciences ClonTech Labs, Palo Alto, California; now available at the American Type Culture Collection, Manassas, Virginia), were maintained at standard growth conditions (37 °C; 95:5 air:CO<sub>2</sub>) using 1:1 DMEM/F12 media containing 10% fetal bovine serum, antibiotics, and 10-mM HEPES buffer (pH 7.4). Cells used in laser exposure experiments were seeded in 96-well plates at 27,000 cells per well, pigmented the following day with isolated bovine MP,<sup>12</sup> and exposed (or used as controls) on the second day post-seed. Adhering to this schedule (seed wells with cells, add melanosomes, and expose to laser, each on consecutive days) provided monolayers with consistent cell density with >95% viability. No residual MP were found in the growth medium after incubation with the RPE cells. This led to our conclusion that there were approximately tenfold more intracellular melanosomes after incubation with stock volumes equivalent to 1600 MP/cell compared to 160 MP/cell.

Cells were exposed to lasers with 200  $\mu$ L Hank's Balanced Salt Solution (HBSS) in each well. After exposure to lasers, this HBSS was replaced with complete growth medium, and the cells were placed at standard culture conditions for 1 h. Finally, cells were assayed for viability using 1.7- $\mu$ M calcein-AM and 1.4- $\mu$ M Ethidium homodimer 1 (EthD1) in 0.04 mL HBSS (10 min at 37 °C). Laser-damaged sites within wells were identified as positively stained when nuclei were fluorescent with EthD1 (bandpass exciter of 475 to 545 nm and a barrier filter at 590 nm) and as a region devoid of staining by calcein-AM (bandpass exciter of 460 to 490 nm and a bandpass emitter of 490 to 530 nm). Scoring of damage by three individuals was blind of dosimetry, and a score (yes/no) for damage required a consensus from two. These binary data were input into the Probit software package.<sup>13</sup> In addition to probability-dose information (ED<sub>50</sub>), the Probit output includes uncertainty intervals (fiducial limits at 95% confidence) related to the ED value, and the Probit slope (first derivative at a probability of 0.5 for ED<sub>50</sub>).

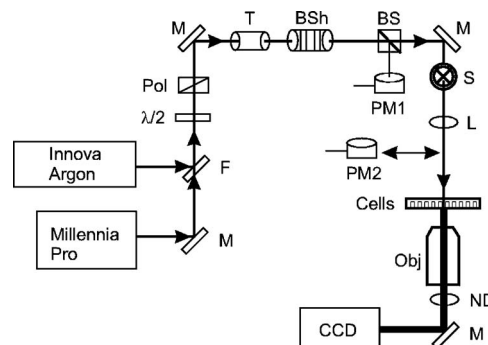


**Fig. 1** Laser delivery for *in vitro* damage threshold experiments. M, mirror; F, flip-up mirror; Pol, polarizing cube; T, optical telescope; BSh, beam shaper; S, shutter; L, lens; PM, power meter; ND, neutral density filter; CCD, charge-coupled device camera; Obj, microscope objective.

### 2.2 Lasers, Beam Delivery, and Cell Exposures

A large-frame argon laser (Innova 200, Coherent) was used for its 457.9-nm line (referred to hereafter as 458 nm). A diode-pumped ND:YVO<sub>4</sub> laser (Millennia Xs, Spectra Physics), with intracavity doubling, was used for the 532-nm exposures.

Figure 1 provides a schematic representation of the laser delivery to cells in the 96-well plates. Attenuation of laser power was achieved by the combination of a half-wave plate ( $\lambda/2$ ) and polarizing beamsplitter (Pol). All beams were then coaligned to a common optical path using apertures and a flip-up mirror (F). The optical path included a telescope (T), a beam shaper (BSh, model GBS-AR14, Newport Corporation), a computer-controlled shutter (S), and a single lens (L) imaging system (88-mm focal length) generating a beam diameter of about 250  $\mu$ m at the cells. The telescope allowed for collimated beam expansion to 4.7 mm prior to entry into the beam shaper, which converted the beam to a flat-top profile. The imaging system was designed to image the beam at the near-field output of the beam shaper (8-mm diam) via 0.05  $\times$  magnification. The effect of the column of HBSS above the cells during exposure was taken into account when identifying laser beam diameter (knife-edge method).

Cells were systematically exposed to laser irradiation for time intervals between 0.1 s and 100 s at irradiance ranges useful for determining viability thresholds. The 96-well plates were suspended (without lids) in the beam path using a specialized holder attached to *x-y* translational stages equipped with computer-controlled motors. Ambient temperatures during the experiments ranged from 18 °C to 25 °C.

### 2.3 Statistics

Uncertainty in our irradiance values was determined from calculated combined standard uncertainties (types A and B) for measuring both laser power and diameter at the sample.<sup>14</sup> The expanded uncertainties in our irradiance values, using a 95% confidence level (i.e., 2 $\times$  standard deviation), ranged from 6% to 7%. Damage threshold irradiance values (ED<sub>50</sub>) were determined using the Probit<sup>15</sup> method. The Probit output includes additional uncertainty intervals (fiducial limits) related

**Table 1** *In vitro* cytotoxicity thresholds in hTERT-RPE1 cells given MP equivalent to 160/cell.

Exposure Duration (s)	Wavelength (nm)	Number of Samples	Probit Slope at ED <sub>50</sub>	ED <sub>50</sub> (W/cm <sup>2</sup> )	Radiant Exposure (J/cm <sup>2</sup> )		
					ED <sub>50</sub>	Lower fiducial limit	Upper fiducial limit
0.1 s	532	19	31.0	664±47	66±5	50±4	74±5
	458	58	11.8	479±33	48±3	42±3	55±4
1.0 s	532	23	12.3	508±32	508±32	403±25	622±39
	458	44	6.2	305±19	305±19	264±17	391±25
10 s	532	20	11.9	347±22	3472±220	2608±165	4611±292
	458	46	13.0	250±16	2502±159	2245±143	2973±189
100 s	532	58	7.8	194±12	19417±1230	16667±1056	22278±1411
	458	63	8.8	53±3	5266±333	3905±247	6122±388

Data are expressed as irradiance ± extended uncertainty or radiant exposure ± extended uncertainty. Extended uncertainty is defined as combined standard uncertainty × *k*, where *k*=2 for 95% confidence.

**Table 2** *In vitro* cytotoxicity thresholds in hTERT-RPE1 cells given MP equivalent to 1600/cell.

Exposure Duration (s)	Wavelength (nm)	Number of Samples	Probit Slope at ED <sub>50</sub>	ED <sub>50</sub> (W/cm <sup>2</sup> )	Radiant Exposure (J/cm <sup>2</sup> )		
					ED <sub>50</sub>	Lower fiducial limit	Upper fiducial limit
1.0 s	532	58	14.1	59±4	59±4	51±3	69±4
	458	39	12.2	73±5	73±5	61±4	84±5
10 s	532	47	24.4	50±3	503±32	422±27	572±36
	458	41	33.5	53±3	526±34	446±29	605±39
100 s	532	48	17.3	33±2	3333±211	2806±178	4028±255
	458	48	13.5	43±3	4264±270	3736±237	4760±301

Data are expressed as irradiance ± extended uncertainty or radiant exposure ± extended uncertainty. Extended uncertainty is defined as combined standard uncertainty × *k*, where *k*=2 for 95% confidence.

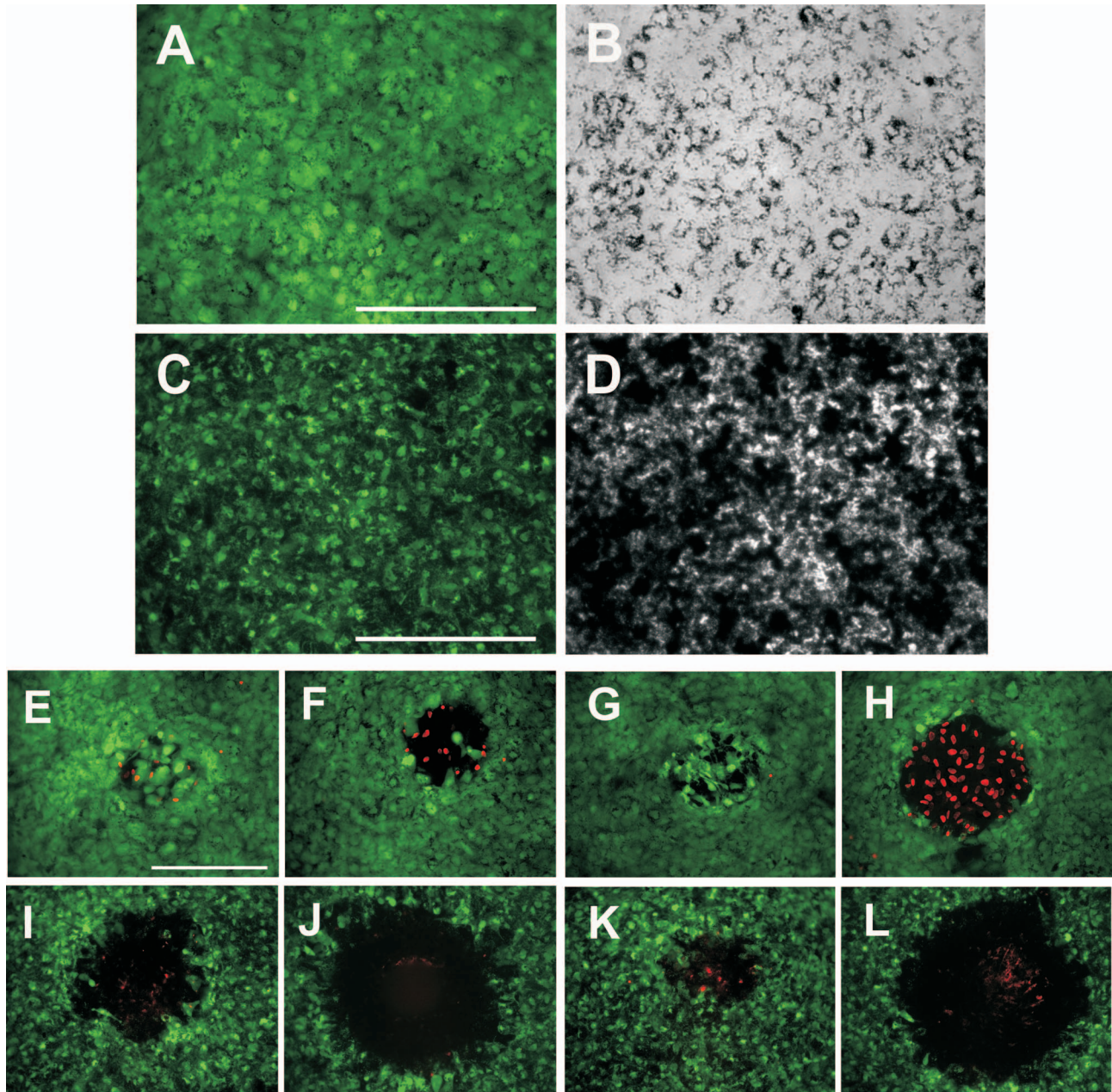


**Fig. 2** Microscopic analysis of RPE pigmentation and laser damage. Panels (a) to (d) represent unexposed hTERT-RPE1 monolayers at 160 MP/cell [(a) and (b)] and 1600 MP/cell [(c) and (d)]. Images were either bright field [(b) and (d)] or stained for viability [(a) and (c)]. Panels (e) to (l) represent cells stained for viability after laser exposure at 458 nm [(e), (f), (i), (j)] or 532 nm [(g), (h), (k), (l)]. Pigmentation of exposed cells was either 160 MP/cell [(e) to (h)] or 1600 MP/cell [(i) to (l)]. Laser irradiances ( $W/cm^2$ ) were as follows: (e), 40; (f), 60, (g), 200; (h), 500; (i), 30; (j), 80; (k), 50; (l), 120. All images were acquired using a 20 $\times$  objective and images (a) to (d) were enlarged to show detail. All spatial bars represent 250 microns.

to the ED<sub>50</sub> value, for which 95% confidence levels also were used. Tables 1 and 2 summarize our threshold results.

### 3 Results

#### 3.1 Laser Damage Thresholds

Figures 2(a) to 2(d) show fluorescence [panels (a) and (c)] and bright field [panels (b) and (d)] images for each of the two levels of pigmentation in our hTERT-RPE1 cells. As expected, there was substantially more pigmentation distributed

throughout the monolayer when adding more melanosomes. Because we saw no residual MP after the phagocytosis period, we expect the two levels of pigmentation to be about tenfold different. Also note that there was sufficient calcein-AM dye in the cells containing the high density of MP to assay for damage. Figures 2(e) to 2(l) provide representative fluorescence images (overlay of red and green channels) for the laser exposures used in our threshold determinations. Note the altered fluorescent staining pattern (red and devoid of green) in the center of the image, indicating cell injury in the region of

**Table 3** Pigment dependence of laser-induced cytotoxicity *in vitro*.

Exposure condition	Fold reduction in ED <sub>50</sub> ( $\frac{160 \text{ MP/cell}}{1600 \text{ MP/cell}}$ )
532 nm	
100 s	5.9
10 s	6.9
1 s	8.6
458 nm	
100 s	1.2
10 s	4.7
1 s	4.2

the monolayer exposed to the damaging effects of a laser.

Damage threshold (ED<sub>50</sub>) values for various laser exposure conditions are listed for hTERT-RPE1 cells pigmented with doses of MP equivalent to 160 MP/cell (Table 1) and 1600 MP/cell (Table 2). Irradiance and radiant exposure thresholds are listed in the tables, but the Probit output data are provided only for the analysis of radiant exposure. Overall, the Probit results indicated statistical confidence in the data sets for each exposure condition. Fiducial limits (representing 95% confidence intervals) within each data set were 5% to 33% from their respective ED<sub>50</sub> value.

For exposures to cells containing 160 MP/cell, the damage thresholds over the 1-s to 100-s range of exposure durations for 458 nm were consistently lower than those for 532 nm. This trend indicates enhanced killing efficiency by exposure to the shorter wavelength, except at the 0.1-s duration. Irradiance thresholds within each wavelength decreased as exposure durations were extended, while the radiant exposure thresholds increased.

Trends for thresholds in cells containing 1600 MP/cell were different from those described for cells with 160 MP/cell. The thresholds for exposure to 532 nm were consistently lower over the range of exposure durations than those for 458 nm, indicating that the longer wavelength was more efficient at killing cells. This pigment-dependent difference in efficiency was especially apparent at the 100-s data point, where the fold-difference between 458 nm and 532 nm was 3.7 (160 MP/cell) and 0.77 (1600 MP/cell).

Table 3 summarizes the pigment-dependent changes in the laser damage threshold. In all conditions compared, a reduction in threshold was found when the pigment density was increased tenfold. The pigment dependence appeared to be less pronounced at the shorter wavelength. The longer exposure duration had the most dramatic effect between the two wavelengths (4.9-fold). Within each wavelength, the general trend was for the pigmentation dependence to be more pronounced at the shorter exposure durations.

Figures 3–5 summarize our data as temporal action profiles, where radiant exposure was plotted versus exposure duration on log-log axes, and which allowed for comparisons

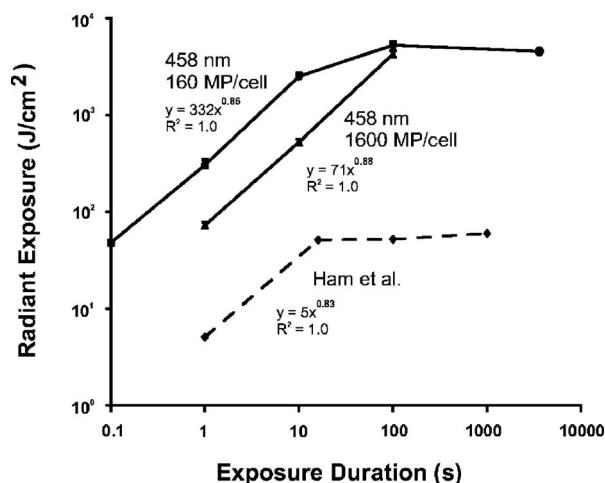


**Fig. 3** Temporal action profiles for *in vitro* thresholds and *in vivo* (Ref. 2) thresholds at 458 nm. The equations (power function with  $R^2$  correlation coefficient) provided in the figure represent only those data corresponding to the linear trends (log-log plot) in each data set. The data point for 160 MP/cell 3600 s is taken from Denton et al.<sup>10</sup>

with *in vivo* laser damage studies reported in the literature. Figure 3 shows our 458-nm temporal action profile in comparison with that from Ham et al.<sup>2</sup> To extend our *in vitro* data set to 3600 s, we have included a data point from an earlier publication.<sup>10</sup> Our *in vitro* thresholds in cells containing 160 MP/cell showed a trend with a striking resemblance to the *in vivo* data. Both curves increased linearly (log-log plot) over the shorter exposure durations (up to and including 10 s), and both leveled off with respect to radiant exposure for the longer exposures (10 s and longer). This occurrence has been termed “reciprocity”<sup>5</sup> and indicates a change in damage mechanisms from one predominately thermal to one that is more photochemical in nature. The trend for *in vitro* exposure of cells having greater pigmentation did not show reciprocity at the 100-s duration point.

When best-fit equations for a power function were determined for the linear portions (log-log plot) of the three curves in Fig. 3, it was found that the slopes (exponents) were similar in magnitude (0.86). The data for the *in vitro* exposures in Fig. 3 showed the pigment-dependent reduction in threshold values for cells containing more MP. The comparison also explained the apparent lack of a pigment dependence at 100 s for the 458-nm exposures as being due to no reciprocity at the higher level of pigmentation.

Because there have been no threshold studies reported in animals for ocular laser exposures at 532 nm, we have made comparisons with studies using 514.5 nm and 580 nm. Figure 4 makes comparisons with 514.5 nm and 580 nm taken from Ham et al.<sup>2</sup> Both *in vitro* temporal action profile curves (power function) were linear (log-log plot) over the 100-s exposure duration, with average slopes of approximately 0.85. The *in vivo* data representing 580-nm exposures gave a linear temporal action profile (log-log plot) over the 1000-s range (slope of 0.73), whereas the data for 514.5-nm exposures showed reciprocity (10 s to 1000 s). Between the 1-s and 10-s data points for the 514.5-nm exposures, the slope was 0.88. From Ham’s data in Fig. 4, the wavelength transition for

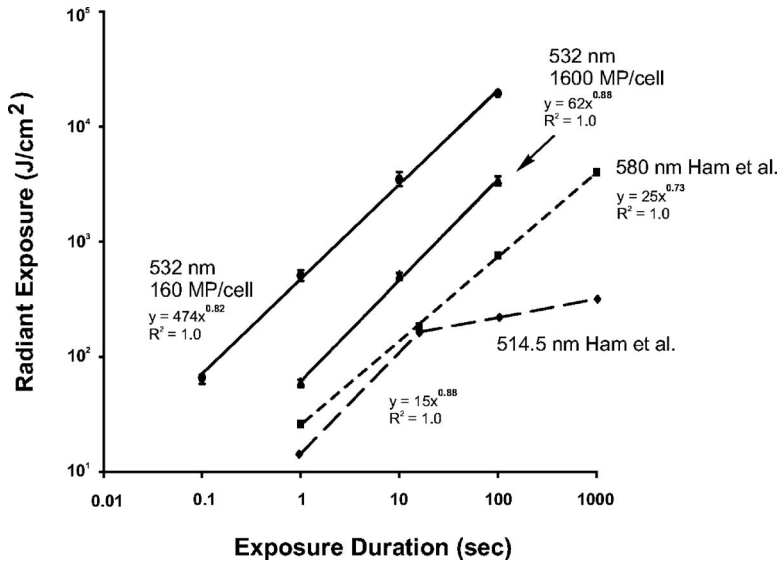


**Fig. 4** Temporal action profiles for *in vitro* (532 nm) thresholds and *in vivo* (580 nm and 514.5 nm from Ref. 2) thresholds. The equations (power function with  $R^2$  correlation coefficient) provided in the figure represent only those data corresponding to the linear trends (log-log plot) in each data set.

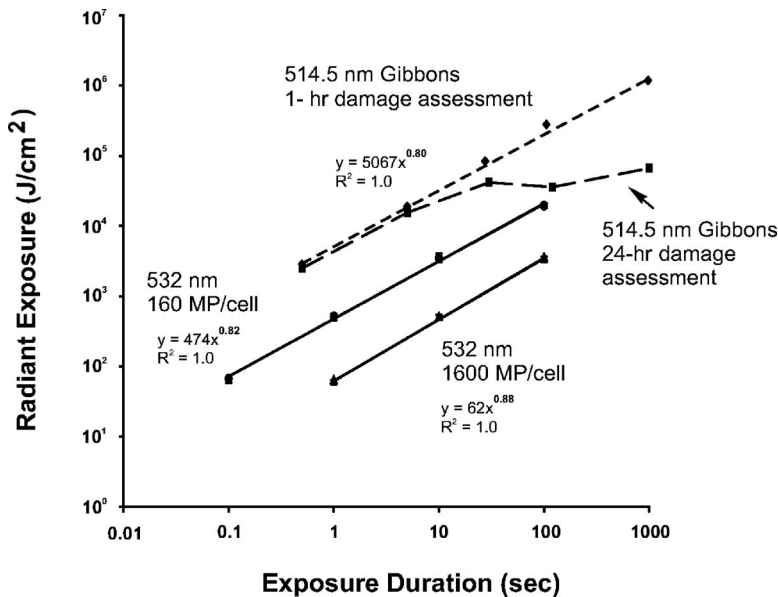
achieving reciprocity *in vivo* fell somewhere between 514.5 nm and 580 nm. Our *in vitro* data would suggest that this transition occurs at a wavelength shorter than 532 nm. Although Figs. 3 and 4 suggest that conditions in the intact eye lead to greater sensitivity for damage from laser exposure, we provide other explanations in Sec. 4.

Figure 5 shows 514.5-nm data from a different animal MVL study<sup>16</sup> for comparison with our 532-nm exposures. Again, the slope of the power function equation for the animal data (0.80) approximated our *in vitro* data at 532 nm. Unlike the 48-h post-exposure data points given by Ham et al.,<sup>2</sup> Gibbons and Allen<sup>16</sup> assessed for damage at both 1 h and 24 h

post-exposure. The extended time of recovery after 514.5-nm exposure was sufficient to allow cells to respond and follow the principle of reciprocity, presumably increasing the degree of photochemical damage relative to thermal damage.

#### 4 Discussion

Our goal was to identify a cellular model that metabolically reacts to laser exposure similarly to RPE cells in nonhuman primate models. Our approach was to determine threshold (ED<sub>50</sub>) radiant exposures for damage over a broad range of durations of exposure and compare with animal (*in vivo*)



**Fig. 5** Temporal action profiles for *in vitro* (532 nm) thresholds and *in vivo* (514.5 nm from Ref. 15) thresholds. The equations (power function with  $R^2$  correlation coefficient) provided in the figure represent only those data corresponding to the linear trends (log-log plot) in each data set.

thresholds reported in the literature. We found that our threshold values differed from two animal studies, most likely because of differences in several exposure parameters that are discussed later. We contend that validation of our model system should primarily focus on how it responds to varying pigmentation, wavelength, and exposure duration (i.e., trends in the threshold data). As described in Sec. 1, threshold trends for *in vivo* exposures indicative of transitions from photothermal to photochemical damage mechanisms have been correlated with calculated temperature-rise data, thus making such comparisons between *in vivo* and *in vitro* threshold trends meaningful.

Our data showed an increase in sensitivity to laser exposure at both 458 nm and 532 nm when intracellular melanosome density in our hTERT-RPE1 cells is increased. The trend (8.6-fold) was most prominent at exposure conditions most consistent with thermal damage (longer wavelength and shortest exposure duration). This type of trend was not evident (1.2-fold) at conditions consistent with photochemical damage (shorter wavelength and longest exposure duration), although Fig. 3 shows that this is because reciprocity had not yet occurred (100 s) for cells having the higher pigmentation.

Thresholds for cells having both levels of pigmentation followed the general trend, where less irradiance was required as exposure duration was extended. When expressed in a temporal action profile, threshold radiant exposure increased as described by a power function. Within each wavelength, the slope (exponent of equation) for the 1600 MP/cell thresholds was slightly greater than the slope for the 160 MP/cell thresholds, which is expected considering the results shown in Table 3. One surprising result was how the ED<sub>50</sub> values for exposures to cells with 1600 MP showed an opposite trend with respect to wavelength. Notice in Table 2 that the 532-nm thresholds were lower than the 458-nm thresholds for each given exposure duration.

Among our *in vitro* damage threshold analyses, only results from exposures to RPE cells containing 160 MP/cell revealed significant features in common with data taken from animal studies in the literature (Figs. 3–5). At this level of artificial pigmentation, the transition to reciprocity for exposure to 458 nm (Fig. 3), but not 532 nm (Fig. 5), for our 1-h post-exposure endpoints was considered supportive of our *in vitro* model. Because the 1600 MP/cell system failed to follow reciprocity (458 nm) or increased sensitivity at the shorter wavelength, we do not consider it a good universal model for studying laser bioeffects. Another positive feature found in Fig. 3 was how the transition from thermal to photochemical damage occurred at around the 20-s exposure duration for both the *in vitro* and *in vivo* exposures at 458 nm.

The data in Figs. 4 and 5 support the notion that our *in vitro* system (160 MP/cell) responds in a fundamentally similar fashion to 532-nm laser irradiation, as does the non-human primate retina. Combined, the *in vivo* data in Figs. 4 and 5 predict that a break point for photochemical damage mechanisms occurs at or around 514 nm and is dependent upon whether one assesses for acute (1-h post-exposure) or chronic (minimum of 24-h post-exposure) damage. From the data trends shown, the presumed thermal response of the hTERT-RPE1 cells exposed to 532 nm complied with expected results in the animal model.

Additionally, the data found in Figs. 3–5 serve to highlight the importance of our analyses of data trends, rather than the absolute values for thresholds at each wavelength and exposure duration. Our thresholds fell consistently above the values from Ham et al.<sup>2</sup> and below those of Gibbons and Allen.<sup>16</sup> We attribute the discrepancies to differences in experimental parameters. For example, Ham et al. did not use the Probit analysis for identifying their thresholds the way it was done in both this study and that of Gibbons and Allen. Rather, Ham et al. determined the lowest irradiance that led to an ophthalmoscopically observable lesion 48 h post-exposure. This would obviously lead to a lower threshold value than the estimated dose that is predicted to produce a lesion 50% of the time (ED<sub>50</sub>). We have already made note of the effect of extending the time of examination for damage, which allows for added physiological responses, typically decreases thresholds in the retina, and is expected to be more pronounced for photochemical damage mechanisms. In regard to the data of Gibbons and Allen that we used in Fig. 5, uncertainty has arisen regarding their ability to image a small laser beam to the same spot at the retina for such extended lengths of time. A “wobble” of the beam would lead to an increase in the power required to achieve damage;<sup>17</sup> however, it is difficult to make direct comparisons when only one group determines ED<sub>50</sub> values.

Some basic physical properties that differed between our *in vitro* experiments and the animal studies reported in the literature include laser beam profile, ambient temperatures during exposure, and the depth and composition of materials preceding the RPE cells. The difference between average and maximum threshold irradiances for the flat-top beam profiles used in our study is minimal compared to the difference for the Gaussian beam profiles used by Ham et al. This alone could account for about a twofold difference in threshold value. Initial temperature of exposed tissue would influence dose requirements to achieve both thermal and photochemical damage (threshold) to cells. A lower initial temperature (such as the 18 °C to 25 °C used in our cell culture experiments), relative to retinal (“body”) temperature of the nonhuman primate is expected to increase the required laser dose to achieve the temperature rise associated with thermal damage. The known temperature dependence of all chemical reactions (rate doubles with each increase of 10 °C) would also predict an increase in threshold laser dose for exposures at lower ambient temperatures. Ongoing experiments in our laboratory are designed to examine these temperature-dependent effects on the laser damage threshold in cultured cells.

Last, the depth and composition of liquid media and tissues that the laser beam must pass through before reaching the RPE cells differed greatly between the cell culture method and the intact globe. The cell culture method eliminated much of the scattering that occurs when light passes through the various layers of the eye. Indeed, we have begun an assessment of the effects of both buffer depth and presence of macular carotenoids in our model system in an effort to aid computational modeling of exposures of blue laser light to the paramacula and macula.

We conclude that the artificially pigmented system described (hTERT-RPE1 cells at 160 MP/cell) is a good model for studying laser bioeffects, although subtle modification in pigmentation may optimize results relative to MVL data.

Wavelength and exposure duration trends in our data indicate that our artificially pigmented RPE cells respond to laser dosimetry via fundamentally similar mechanisms when compared to native RPE cells. The cell culture model has an easily manipulated environment, provides laser delivery with relative ease, and can generate large data sets quickly.

### Acknowledgments

The opinions, interpretations, conclusions, and recommendations are those of the authors and are not necessarily endorsed by the U.S. Air Force. We thank D. Stolarski and G. Noojin for technical assistance. This work was supported by the Air Force Office of Scientific Research, Grant No. 92HE04COR.

### References

1. W. T. Ham Jr., J. J. Ruffolo Jr., H. Mueller, and D. Guerry III, "The nature of retinal radiation damage: dependence on wavelength, power level, and exposure time," *Vision Res.* **20**, 1105–1111 (1980).
2. W. T. Ham Jr., H. A. Mueller, M. J. Ruffolo Jr., and A. M. Clarke, "Sensitivity of the retina to radiation damage as a function of wavelength," *Photochem. Photobiol.* **29**, 735–743 (1979).
3. W. T. Ham Jr., J. J. Ruffolo Jr., H. A. Mueller, A. M. Clarke, and M. E. Moon, "Histologic analysis of photochemical lesions produced in rhesus retina by short-wavelength light," *Invest. Ophthalmol. Visual Sci.* **17**, 1029–1035 (1978).
4. B. E. Stuck, "The retina action spectrum for photoreinitis ('blue-light hazard')," in *Measurements of Optical Radiation Hazards*, D. Sliney, Ed., pp. 193–208, ICNIRP 6/98, CIEx016-1998, Maerkl-Druck, Munich (1998).
5. G. A. Griess and M. F. Blankenstein, "Additivity and repair of actinic retinal lesions," *Invest. Ophthalmol. Visual Sci.* **20**, 803–807 (1981).
6. W. T. Ham Jr. and H. A. Mueller, "The photopathology and nature of the blue light and near-UV retinal lesions produced by lasers and other optical sources," in M. L. Wolbarsht, Ed., pp. 191–246, *Laser Applications in Medicine and Biology*, Plenum Publishing, New York (1989).
7. A. M. Clarke, W. J. Geeraets, and W. T. Ham, "An equilibrium thermal model for retinal injury from optical sources," *Appl. Opt.* **8**, 1051–1054 (1969).
8. A. N. Takata, L. Goldfinch, J. K. Hinds, L. P. Kuan, N. Thomopoulos, and A. Weigandt, "Thermal model of laser-induced eye damage," *Engr. Mech. Div., IIT Res Institute, Technical Report IITRI J-TR-74-6324* (available from NTIS, Springfield, VA, as AD-A017 201) (1974).
9. T. X. Pedersen, C. Leethanakul, V. Patel, D. Mitola, L. R. Lund, K. Dano, M. Johnsen, J. S. Gutkind, and T. H. Bugge, "Laser capture microdissection-based *in vivo* genomic profiling of wound keratinocytes identifies similarities and differences to squamous cell carcinoma," *Oncogene* **22**, 3964–3976 (2003).
10. M. L. Denton, M. S. Foltz, L. E. Estlack, D. J. Stolarski, G. D. Noojin, R. J. Thomas, D. Eikum, and B. A. Rockwell, "Damage threshold for exposure to NIR and blue lasers in an *in vitro* RPE cell system," *Invest. Ophthalmol. Visual Sci.* **47**, 3065–3073 (2006).
11. M. L. Denton, D. M. Eikum, G. D. Noojin, D. J. Stolarski, R. J. Thomas, R. D. Glickman, and B. A. Rockwell, "Pigmentation in NIR laser tissue damage," in *Laser and Noncoherent Light Ocular Effects: Epidemiology, Prevention, and Treatment*, B. E. Stuck and M. Belkin, Eds., *Proc. SPIE* **4953**, 78–84 (2003).
12. A. E. Dontsov, R. D. Glickman, and M. Ostrovsky, "Retinal pigment epithelium pigment granules stimulate the photo-oxidation of unsaturated fatty acids," *Free Radic Biol. Med.* **26**, 1436–1446 (1999).
13. C. P. Cain, G. D. Noojin, and L. Manning, "A comparison of various probit methods for analyzing yes/no data on a log scale," USAF School of Aerospace Medicine, Brooks Air Force Base, TX, USAF Technical Report AL/OE-TR-1996-0102 (available from NTIS, Springfield, VA, as AD-A319 412/3) (1996).
14. B. N. Taylor and C. E. Kuyatt, "Guidelines for evaluating and expressing the uncertainty of NIST measurement results," NIST Tech. Note 1297 (1994).
15. D. J. Finney, *Probit Analysis*, Cambridge University Press, New York (1971).
16. W. D. Gibbons and R. G. Allen, "Retinal damage from long-term exposure to laser radiation," *Invest. Ophthalmol. Visual Sci.* **16**, 521–529 (1977).
17. D. H. Sliney, J. Mellerio, V.-P. Gabel, and K. Schulmeister, "What is the meaning of threshold in laser injury experiments? Implications for human exposure limits," *Health Phys.* **82**, 335–347 (2002).